Poisson-Boltzmann Theory of Charged Colloids: Limits of the Cell Model for Salty Suspensions

A. R. Denton†

Dept. of Physics, North Dakota State University, Fargo, ND, U.S.A. 58108-6050

Abstract. Thermodynamic properties of charge-stabilised colloidal suspensions and polyelectrolyte solutions are commonly modeled by implementing the mean-field Poisson-Boltzmann (PB) theory within a cell model. This approach models a bulk system by a single macroion, together with counterions and salt ions, confined to a symmetrically shaped, electroneutral cell. While easing numerical solution of the nonlinear PB equation, the cell model neglects microion-induced interactions and correlations between macroions, precluding modeling of macroion ordering phenomena. An alternative approach, which avoids the artificial constraints of cell geometry, exploits the mapping of a macroion-microion mixture onto a one-component model of pseudo-macroions governed by effective interparticle interactions. In practice, effective-interaction models are usually based on linear-screening approximations, which can accurately describe strong nonlinear screening only by incorporating an effective (renormalized) macroion charge. Combining charge renormalization and linearized PB theories, in both the cell model and an effective-interaction (cell-free) model, we compute osmotic pressures of highly charged colloids and monovalent microions, in Donnan equilibrium with a salt reservoir, over a range of concentrations. By comparing predictions with primitive model simulation data for salt-free suspensions, and with predictions of nonlinear PB theory for salty suspensions, we chart the limits of both the cell model and linear-screening approximations in modeling bulk thermodynamic properties. Up to moderately strong electrostatic couplings, the cell model proves accurate in predicting osmotic pressures of deionized (counterion-dominated) suspensions. With increasing salt concentration, however, the relative contribution of macroion interactions to the osmotic pressure grows, leading predictions of the cell and effective-interaction models to deviate. No evidence is found for a liquid-vapour phase instability driven by monovalent microions. These results may guide applications of PB theory to colloidal suspensions and other soft materials.

PACS numbers: 82.70.Dd, 83.70.Hq, 05.20.Jj, 05.70.-a

† Electronic address: alan.denton@ndsu.edu

1. Introduction

When dispersed in water, or other polar solvents, colloidal particles can acquire an electric charge through surface dissociation of counterions [1]. Electrostatic repulsions between charged macroions, screened by surrounding microions (counterions, salt ions), act to stabilise colloidal suspensions against aggregation induced by attractive van der Waals forces, as first explained by the classic theory of Derjaguin, Landau, Verwey, and Overbeek (DLVO) [2, 3]. Equilibrium and dynamical properties of many soft and biologically prevalent materials, including charge-stabilised colloids, polyelectrolytes, and ionic surfactants, are largely determined by microion distributions and induced electrostatic interactions between macroions.

Molecular simulations provide essentially exact results for model colloidal suspensions and polyelectrolyte solutions, but can access only limited parameter ranges of these complex systems. For salt-free suspensions, recent Monte Carlo studies of the primitive model have probed osmotic pressure, thermodynamic stability, and macroion structure [4, 5, 6, 7, 8, 9] and characterized effective macroion interactions [10, 11, 12, 13, 14] and bulk phase behaviour, including liquid-vapour separation [15, 16, 17] and melting [18]. At significant salt concentrations, proliferation of microions renders simulations of the primitive model unwieldy, and data for bulk properties of salty suspensions are scarce.

Materials with strong electrostatic interparticle interactions [19] are commonly modeled via Poisson-Boltzmann (PB) theory [20, 21], which combines the exact Poisson equation for the electrostatic potential with a mean-field (Boltzmann) approximation for the microion densities. Neglect of correlations between microions is strictly justifiable only for weak electrostatic couplings, characteristic of monovalent microions in water. Nevertheless, the mean-field PB theory often makes at least qualitatively correct predictions for thermodynamic properties and provides a valuable reference for simulations and more sophisticated theories that incorporate correlations.

Central to Poisson-Boltzmann theory is the PB equation governing the electrostatic potential. For symmetric (isotropic) boundary conditions, this nonlinear differential equation is easily solved — analytically in planar and cylindrical geometries, and numerically in spherical coordinates. For this reason, PB theory is most often implemented within a cell model [21, 22], which reduces a bulk suspension to a single macroion — idealised as a charged sphere, rod, or plate — centred in a cell of the same shape, together with salt ions and neutralizing counterions. While a symmetric cell may reasonably approximate the Wigner-Seitz cell of a periodic crystal, the computational advantage gained by imposing symmetry is offset by a loss of accuracy in neglecting microion-induced interactions and correlations between macroions. Although efficient for modeling nonlinear microion screening, the cell model is not designed to describe macroion structure and ordering.

An alternative theoretical approach, which strives to incorporate macroion structure, maps the multi-component ion mixture onto a one-component model by

averaging over microion degrees of freedom in the partition function [23]. The resulting pseudo-macroions are governed by an effective Hamiltonian involving effective electrostatic interactions. Although the one-component model is free of the constraints of cell geometry, practical implementation usually requires invoking linear-screening approximations, derived by linearizing the PB equation. Moreover, in applying linearized theories to strongly-coupled suspensions of highly charged macroions, it proves essential to consistently incorporate an effective (renormalized) macroion charge to properly account for nonlinear microion screening [24, 25, 26, 27].

Condensation of counterions onto highly charged polyelectrolyte chains is well established [28, 29]. By comparison, the association of counterions with spherical macroions is a rather more subtle and less understood phenomenon. Several theories have been proposed to describe counterion accumulation around highly charged macroions and the resulting reduction of the effective macroion valence. In a pioneering study, Alexander *et al.* [30] defined an effective macroion valence for the Debye-Hückel (linear-screening) theory by matching solutions of the nonlinear and linearized PB equations at the boundary of a spherical cell. In a series of studies, Levin and coworkers applied liquid-state theory [31, 32, 33] and derived an effective valence from a jellium approximation [34, 35, 36, 37] for the total free energy. Other thermodynamic approaches are based on a thermal criterion for either the electrostatic potential around a macroion [38, 39, 40] or the effective pair potential [41]. Recently, an effective valence has been incorporated into the one-component model with linear-screening effective interactions [42, 43, 44, 45].

Effective macroion charges have been measured in experiments, e.g., by torsional resonance spectroscopy [46], light or small angle neutron scattering [47, 48], and conductivity [49] measurements. Renormalized charges also have been extracted from Monte Carlo (MC) simulations according to various criteria: equating the Debye-Hückel pressure [10] or chemical potential [50] to the corresponding MC quantity; applying the prescription of Alexander *et al.* [30] to the spherical cell model [6]; fitting an effective Yukawa pair potential by inverting the macroion-macroion pair distribution function [13]; from the inflection point of the curve of accumulated running charge vs. inverse separation from the macroion centre [14, 51]; and from a dynamical criterion relating the counterion kinetic and potential energies [52].

The purpose of this paper is twofold: first, to generalize the charge renormalization theory proposed in ref. [44] from salt-free suspensions to suspensions dialyzed against an electrolyte reservoir; second, to apply the generalized theory to salty suspensions to test the accuracy of the PB cell model in predicting osmotic pressure over a wide range of salt concentrations. By comparing results with available simulation data for deionized suspensions and with predictions of nonlinear PB theory for salty suspensions, we explore the limits of both the cell model and linearization approximations in predicting bulk thermodynamic properties. Up to moderately strong electrostatic couplings, the cell model proves accurate in predicting osmotic pressures of counterion-dominated suspensions (low salt concentrations). With increasing salt concentration, as macroion

interactions gain in relative importance, predictions of the one-component (effective-interaction) model increasingly deviate from those of the cell model. No evidence is found of a liquid-vapour spinodal instability for a physically rational definition of the renormalization threshold.

The paper is organized as follows. Section 2 first reviews the relevant models: the primitive model of charged colloids, the charge renormalization model for the effective macroion valence, and the one-component model governed by an effective Hamiltonian. Working from the density-functional formulation of Poisson-Boltzmann theory, Sect. 3 then derives the PB equation and outlines the two main implementations: the cell model and the effective-interaction model. In Sect. 4, the two implementations of PB theory are linearized about the mean potential or, equivalently, the mean microion densities. Section 5 applies the nonlinear and linearized PB theory to calculate the osmotic pressure and compares predictions with available data from primitive model simulations of salt-free suspensions. Finally, Sect. 6 summarizes and concludes.

2. Models

2.1. Primitive Model

The primitive model of charged colloids and polyelectrolytes idealises the solvent as a homogeneous dielectric continuum of relative permittivity ϵ. Dispersed throughout the solvent are macroions and microions, here modeled, respectively, as charged hard spheres of radius a and valence Z (charge $-Ze$) and monovalent point ions. In a closed suspension, all particles are confined to the same volume V. In Donnan equilibrium, only the macroions are confined, while the microions can exchange (e.g., across a semi-permeable membrane) with a salt reservoir, here assumed to be a 1:1 electrolyte. Modeling the reservoir as an ideal gas of ions of pair number density n_0, the suspension has fixed salt chemical potential $\mu_s = 2\mu_0$, where $\mu_0 = k_B T \ln(n_0 \Lambda^3)$ is the chemical potential of each microion species at absolute temperature T, the thermal wavelength Λ defining the arbitrary zero of the chemical potential.

A bulk suspension of N_m macroions, N_c counterions, and N_s dissociated pairs of oppositely charged salt ions contains $N_+ = N_c + N_s$ positive and $N_- = N_s$ negative microions, for a total of $N_\mu = N_c + 2N_s$ microions. Global electroneutrality constrains the macroion and counterion numbers by the condition $ZN_m = N_c$. Accounting for excluded-volume and electrostatic (Coulomb) pairwise interparticle interactions, the primitive model Hamiltonian can be expressed as

$$H = H_m + H_\mu + H_{m\mu} \ , \tag{1}$$

which separates naturally into three terms: a macroion Hamiltonian,

$$H_m = H_{\rm hs} + \frac{Z^2 e^2}{2\epsilon} \sum_{i \neq j = 1}^{N_m} \frac{1}{r_{ij}} \ , \tag{2}$$

where $H_{\rm hs}$ is the macroion hard-sphere Hamiltonian (including kinetic energy) and r_{ij} is the centre-centre separation between ions; a microion Hamiltonian,

$$H_\mu = K_\mu + \frac{e^2}{2\epsilon} \sum_{i\neq j=1}^{N_\mu} \frac{z_i z_j}{r_{ij}} \ , \tag{3}$$

with microion valences $z_i = \pm 1$ and kinetic energy K_μ; and a macroion-microion interaction energy,

$$H_{m\mu} = \frac{Ze^2}{\epsilon} \sum_{i=1}^{N_m} \sum_{j=1}^{N_\mu} \frac{z_j}{r_{ij}} \ . \tag{4}$$

2.2. Charge Renormalization Model for Effective Charge

The parameter Z in the primitive model corresponds to the maximum (bare) charge of the macroions, measureable by titration. In practice, this simple correspondence may be complicated by chemical reactions at the macroion surface, dependent on pH and salinity, which can affect ion dissociation [47, 53, 54]. Even in the absence of charge regulation, however, the *effective* macroion charge — probed by electrophoresis, rheology, and scattering experiments — may lie considerably below the bare charge.

The distinction between bare and effective charges arises from the strong association between counterions and highly charged macroions. Planar and rodlike macroions generate electrostatic potentials of sufficiently long range to condense counterions above a threshold surface charge density [28]. In contrast, the potential outside of a spherical macroion decays too rapidly to overcome entropy and irreversibly bind counterions. Nevertheless, counterions that venture sufficiently close to the macroion surface to become thermally (transiently) bound can be considered to renormalize the bare charge to a lower effective charge [30]. The remaining, weakly associated, counterions contribute to screening of the effective charge and are amenable to linear-screening approximations.

Akin to Oosawa's two-phase theory of polyelectrolyte solutions [29], free and bound counterions part ways at a distance from the macroion at which the deviation of the electrostatic energy of counterion-macroion attraction from the average potential energy rivals the typical thermal energy k_BT per counterion. Defining $\psi(r)$ as the reduced electrostatic potential energy (in k_BT units) at distance r from the centre of a macroion, the thickness of the spherical association shell δ (Fig. 1) is defined by the condition

$$|\psi(a+\delta) - \overline{\psi}| = C \ , \tag{5}$$

where $\overline{\psi}$ is the spatially-averaged potential and C is a constant of $\mathcal{O}(1)$ yet to be specified. At distances $r > a + \delta$, the deviation is presumed to be sufficiently small that a linear-screening approximation is valid. Assuming coions to be expelled from the association shell, the "dressed" macroion [55], consisting of a bare macroion and its shell of bound counterions, carries an effective valence $\tilde{Z} \leq Z$. Statistical fluctuations in $\tilde{Z}$ are neglected in this simple model. Other workers have applied a thermal criterion similar to Eq. (5) to the electrostatic potential [38, 39, 40] or the effective pair potential [41].

2.3. One-Component Model and Effective Hamiltonian

Simulations of the primitive model [7, 8] have characterized bulk properties of salt-free (counterion-dominated) suspensions with relatively low charge asymmetry ($Z < 100$). Significant concentrations of salt pose, however, computational challenges for large-scale simulations of bulk suspensions. Consider, for example, that at 10 mM salt concentration a suspension of 100 macroions of radius $a = 10$ nm at 1% volume fraction contains $\mathcal{O}(10^6)$ particles, all interacting via long-range Coulomb forces, and that the particle number scales as a^3. Therefore, salt-dominated suspensions usually are modeled by first mapping the multi-component mixture onto a one-component model (OCM).

In Donnan equilibrium, a suspension is governed by a semigrand partition function,

$$\mathcal{Z} = \langle\langle \exp(-\beta H)\rangle_\mu\rangle_m \ , \tag{6}$$

where $\langle\ \rangle_\mu$ denotes a grand canonical trace over microion coordinates, $\langle\ \rangle_m$ a canonical trace over macroion coordinates, and $\beta \equiv 1/(k_B T)$. The one-component mapping expresses the partition function in the form

$$\mathcal{Z} = \langle \exp(-\beta H_{\rm eff})\rangle_m \ , \tag{7}$$

where the effective Hamiltonian for a one-component system of pseudo-macroions

$$H_{\rm eff} \equiv H_m - k_B T \ln\langle \exp[-\beta(H_\mu + H_{m\mu})]\rangle_\mu \equiv \Omega_\mu \tag{8}$$

can be interpreted equivalently as the grand potential Ω_μ of the microions in the "external" potential of the macroions. For a closed suspension, with fixed microion numbers, $\langle\ \rangle_\mu$ becomes a canonical trace over microion coordinates and Ω_μ is replaced by the Helmholtz free energy of the microions.

Practical applications of the OCM require approximating Ω_μ. For this purpose, Poisson-Boltzmann theory is a powerful approach. Below we briefly review PB theory and two common implementations: the cell model and the effective-interaction approach.

3. Poisson-Boltzmann Theory

3.1. Density-Functional Formulation

Poisson-Boltzmann theory is most elegantly formulated within the framework of classical density-functional theory of nonuniform fluids [56, 57]. Corresponding to the primitive model Hamiltonian [Eqs. (2)-(4)], there exists a Helmholtz free energy functional $F[n_m(\mathbf{r}), n_\pm(\mathbf{r})]$, which (for a given external potential) is a unique functional of the macroion and microion number density profiles, $n_m(\mathbf{r})$ and $n_\pm(\mathbf{r})$, varying with spatial position $\mathbf{r}$. This free energy functional separates, according to $F = F_{\rm id} + F_{\rm ex} + F_{\rm ext}$, into a (purely entropic) ideal-gas free energy functional of all ions,

$$F_{\rm id} = k_B T \int_V {\rm d}\mathbf{r} \sum_{i=m,\pm} n_i(\mathbf{r})\{\ln[n_i(\mathbf{r})\Lambda^3] - 1\} \ , \tag{9}$$

an excess free energy functional, $F_{\rm ex} = F_{\rm hs} + F_{\rm el}$, due to hard-sphere (hs) and electrostatic (el) interparticle interactions, and a contribution $F_{\rm ext}$ due to an external potential.

Neglecting interparticle correlations (mean-field approximation), the electrostatic part of the excess free energy functional may be approximated as

$$F_{\rm el} = \frac{1}{2}\int_V {\rm d}\mathbf{r}\, \rho(\mathbf{r})\Phi(\mathbf{r}) \ , \tag{10}$$

where $\rho(\mathbf{r}) = e[n_+(\mathbf{r}) - n_-(\mathbf{r}) - n_f(\mathbf{r})]$ is the total charge density, including the negative charge fixed on the macroion surfaces of number density $n_f(\mathbf{r})$, and

$$\Phi(\mathbf{r}) = \int {\rm d}\mathbf{r}'\, \frac{\rho(\mathbf{r}')}{\epsilon|\mathbf{r}-\mathbf{r}'|} \tag{11}$$

is the total electrostatic potential at position $\mathbf{r}$ due to all ions. The potential and the total ion density are related via the exact Poisson equation

$$\nabla^2\Phi(\mathbf{r}) = -\frac{4\pi}{\epsilon}\rho(\mathbf{r}) \ , \tag{12}$$

which may be expressed in the form

$$\nabla^2\psi(\mathbf{r}) = -4\pi\lambda_B[n_+(\mathbf{r}) - n_-(\mathbf{r})] \ ; \quad \nabla\psi|_{\rm surface} = Z\lambda_B/a^2 \ , \tag{13}$$

where $\psi \equiv \beta e\Phi$ is the reduced electrostatic potential, $\lambda_B = \beta e^2/\epsilon$ defines the Bjerrum length, and the macroion charges are absorbed into a boundary condition at the macroion surfaces. The microion densities implicitly vanish inside the macroion cores.

For a given external potential, the equilibrium densities of all ions minimize the total grand potential functional of the system. Alternatively, fixing the macroion coordinates and regarding their charges as the source of an external potential, the equilibrium microion densities alone minimize the microion grand potential functional

$$\Omega_\mu[n_\pm(\mathbf{r})] = F_\mu[n_\pm(\mathbf{r})] - \mu_+\int_V {\rm d}\mathbf{r}\, n_+(\mathbf{r}) - \mu_-\int_V {\rm d}\mathbf{r}\, n_-(\mathbf{r}) \ , \tag{14}$$

defined as a Legendre transform of the microion free energy functional

$$F_\mu[n_\pm(\mathbf{r})] = k_BT\int_V {\rm d}\mathbf{r}\, \sum_{i=\pm} n_i(\mathbf{r})\{\ln[n_i(\mathbf{r})\Lambda^3] - 1\} + \frac{1}{2}\int_V {\rm d}\mathbf{r}\, \rho(\mathbf{r})\Phi(\mathbf{r}) \ , \tag{15}$$

the microion (electro)chemical potentials $\mu_\pm$ being identified as the Legendre variables. Note that Ω_μ depends parametrically on the macroion coordinates and that F_μ includes macroion-macroion Coulomb interactions for electroneutrality. Under the assumption that either the electrostatic potential or the electric field vanishes everywhere on the boundary of the volume V, the microion free energy functional also may be expressed in the form

$$\beta F_\mu[n_\pm(\mathbf{r})] = \int_V {\rm d}\mathbf{r}\, \sum_{i=\pm} n_i(\mathbf{r})\{\ln[n_i(\mathbf{r})\Lambda^3] - 1\} + \frac{1}{8\pi\lambda_B}\int_V {\rm d}\mathbf{r}\, |\nabla\psi|^2 \ . \tag{16}$$

Minimizing $\Omega_\mu[n_\pm(\mathbf{r})]$ with respect to $n_\pm(\mathbf{r})$ now yields the mean-field Boltzmann approximation for the equilibrium microion densities

$$n_\pm(\mathbf{r}) = n_\pm^{(0)}\exp[\mp\psi(\mathbf{r})] \quad \text{(fixed macroions)} \ , \tag{17}$$

the reference densities, $n_\pm^{(0)} = \Lambda^{-3}\exp(\beta\mu_\pm)$, being the microion densities at the reference potential $\psi = 0$. Evaluating the microion grand potential functional [Eq. (14)] at the equilibrium microion density profiles [Eq. (17)] yields the microion grand potential

$$\beta\Omega_\mu = -\int_V {\rm d}\mathbf{r}\, [n_+(\mathbf{r}) + n_-(\mathbf{r})] - \frac{1}{2}\int_V {\rm d}\mathbf{r}\, [n_+(\mathbf{r}) - n_-(\mathbf{r}) + n_f(\mathbf{r})]\psi(\mathbf{r}) \ . \tag{18}$$

For a closed suspension (fixed particle numbers), the chemical potentials of the two microion species differ because of asymmetric interactions with the macroions: $\mu_+ \neq \mu_-$. Correspondingly, the reference densities also differ: $n_+^{(0)} \neq n_-^{(0)}$. In Donnan equilibrium, however, exchange of microions with a salt reservoir shifts the intrinsic microion chemical potentials, $\mu_\pm^{\text{in}} = [\delta F_\mu / \delta n_\pm(\mathbf{r})]_{\text{eq}}$, by the Donnan potential ψ_D:

$$\beta\mu_\pm = \beta\mu_\pm^{\text{in}} \pm \psi_D = \beta\mu_0 = \ln(n_0\Lambda^3) \; . \tag{19}$$

The total chemical potentials, and so too the reference densities, of the two microion species are thus equalized. The equilibrium microion density profiles are then given by

$$n_\pm(\mathbf{r}) = n_0 \exp[\mp\psi(\mathbf{r})] \; . \tag{20}$$

The Donnan potential is interpreted physically as the change in electrostatic potential across the reservoir-suspension interface, and mathematically as a Lagrange multiplier for the constraint of global electroneutrality.

Combining the Poisson equation for the potential [Eq. (13)] with the Boltzmann approximation for the microion densities [Eq. (17) or (20)], the Poisson-Boltzmann equation takes the form

$$\nabla^2\psi(\mathbf{r}) = \begin{cases} -4\pi\lambda_B \left(n_+^{(0)} \exp[-\psi(\mathbf{r})] - n_-^{(0)} \exp[\psi(\mathbf{r})] \right) & \text{(closed)} \\ \kappa_0^2 \sinh\psi(\mathbf{r}) \; ; \quad \nabla\psi|_{\text{surface}} = Z\lambda_B/a^2 \; , & \text{(Donnan)} \end{cases} \tag{21}$$

where $\kappa_0 = \sqrt{8\pi\lambda_B n_0}$ is the screening constant in the reservoir. Beyond the boundary condition at the macroion surfaces, the boundary-value problem is fully specified only by imposing another condition at the outer boundary of the system, which depends on the practical implementation of the theory.

3.2. Cell-Model Implementation

The anisotropic boundary conditions on the nonlinear PB equation imposed by an arbitrary configuration of macroions render a general solution of Eq. (21) computationally daunting. In recent years, powerful *ab initio* methods have been developed for combining PB theory of microion density profiles with molecular dynamics [56, 57, 58, 59] or Brownian dynamics [60, 61] simulation to evolve macroion coordinates according to derived forces. Despite such advances, however, most applications of PB theory have been implemented within a cell model to facilitate numerical solution.

In a seemingly bold reduction, the cell model represents a bulk suspension by a single macroion, neutralizing counterions, and salt ions confined to a cell of the same shape as the macroion. Microion-induced interactions between macroions are simply ignored. For spherical colloids, the natural choice is a spherical cell centred on the macroion [62]. Gauss's law then dictates that the electric field must vanish everywhere on the boundary of the electroneutral cell. With the potential and microion densities depending on only the radial coordinate r, the PB equation reduces to an ordinary differential equation for $\psi(r)$ with boundary conditions $\psi'(a) = Z\lambda_B/a^2$ and

$\psi'(R) = 0$, where the cell radius R is commensurate with the average macroion density: $n_m = N_m/V = 3/(4\pi R^3)$. For a closed suspension, the arbitrary location of the reference point of the electrostatic potential (where $\psi = 0$) is usually chosen as the cell boundary: $\psi(R) = 0$. In Donnan equilibrium, the potential is conventionally chosen to vanish in the reservoir, in which case the boundary value of the electrostatic potential is identified as the Donnan potential: $\psi(R) = \psi_D \neq 0$.

An appealing feature of the cell model is the simple analytic relation between the bulk pressure p and the microion densities at the cell boundary:

$$\beta p = n_+(R) + n_-(R) \; . \tag{22}$$

Although first derived within the mean-field PB framework [22], this pressure relation proves to be exact within the cell model [63], i.e., valid also for correlated microions. In Donnan equilibrium with an ideal-gas reservoir, the osmotic pressure Π, i.e., the difference in pressure between suspension and reservoir, is then given by

$$\beta\Pi = n_+(R) + n_-(R) - 2n_0 \; . \tag{23}$$

Within PB theory, the osmotic pressure is strictly positive [26], which follows simply from Eqs. (20) and (23) and the inequality, $\cosh x > 1$.

The cell model implements PB theory by approximating the microion grand potential [Eq. (8)] in the one-component mapping of the primitive model (Sec. 2.3). Reducing a bulk suspension to a single macroion in a symmetrically shaped cell with isotropic boundary conditions greatly facilitates solution of the nonlinear PB equation. The microion grand potential implicitly depends on the average macroion density through the density-dependent cell radius. Moreover, bare Coulomb interactions among all macroions are included in an average sense via the electroneutrality constraint. The cell-model implementation excellently approximates the single-macroion (one-body) contribution to the free energy and pressure. The trade-off for fully incorporating nonlinear microion screening, however, is complete neglect of effective interactions and correlations among macroions induced by microions. Accurately accounting for multi-macroion contributions to thermodynamic properties requires an effective-interaction implementation of PB theory.

3.3. Effective-Interaction Implementation

An alternative implementation of PB theory, also based on the one-component mapping, focuses on effective interactions derived from perturbative expansion of the microion grand potential about a uniform reference system, namely, a plasma of microions unperturbed by the macroions. By incorporating macroion interactions, this approach can model both thermodynamic and structural properties of colloidal suspensions. Several liquid-state theoretical frameworks have been developed. Density-functional theories [64, 65, 66, 67] expand the ideal-gas free energy functional in a Taylor series in powers of deviations of the microion density profiles from their mean values $\bar{n}_\pm$:

$$\beta F_{\rm id}[n_\pm(\mathbf{r})] = \sum_{i=\pm} \left(N_i[\ln(\bar{n}_i\Lambda^3) - 1] + \frac{1}{2\bar{n}_i} \int {\rm d}\mathbf{r} \, [n_i(\mathbf{r}) - \bar{n}_i]^2 + \cdots \right) \; . \tag{24}$$

Response theories [74, 75, 76, 77, 78, 79] expand the microion density profiles about a reference plasma in powers of the macroion potential, $\phi_{m\pm}(\mathbf{r}) = \int \mathrm{d}\mathbf{r}'\, v_{m\pm}(|\mathbf{r}-\mathbf{r}'|)n_m(\mathbf{r}')$:

$$n_i(\mathbf{r}) = \bar{n}_i + \sum_{j=\pm} \int \mathrm{d}\mathbf{r}'\, \chi_{ij}(|\mathbf{r}-\mathbf{r}'|)\phi_{mj}(\mathbf{r}') + \cdots \ , \tag{25}$$

where $\chi_{ij} = \delta n_i(\mathbf{r})/\delta\phi_{mj}(\mathbf{r}')$ are linear response functions of the reference plasma and higher-order terms involve nonlinear response functions. Distribution function theories are based on density-functional expansions of the microion correlation functions about a reference plasma [68, 69, 70, 71, 72, 73] or on integral-equation closures [80, 81, 82, 83, 84, 85, 86].

In all of these statistical mechanical schemes, insertion of the perturbative expansion into Eq. (8) recasts the effective Hamiltonian (microion grand potential) in the form of a sum of effective interactions:

$$H_{\mathrm{eff}} = E_v + H_{\mathrm{hs}} + \frac{1}{2}\sum_{i\neq j=1}^{N_m} v_{\mathrm{eff}}(r_{ij}) + \cdots \ , \tag{26}$$

where E_v is a one-body volume energy – independent of the macroion coordinates but dependent on the average macroion density – $v_{\mathrm{eff}}(r)$ is an effective electrostatic pair potential summed over macroion pairs with centre-centre separation r, and higher-order terms involve sums over effective many-body interactions. The volume energy here corresponds to the microion grand potential for a single macroion.

In practice, mean-field (Debye-Hückel-like) approximations for the electrostatic free energy, response functions, or correlation functions, make the various effective-interaction approaches essentially equivalent. Thermodynamic and structural properties of a bulk system can be calculated by inputting the effective interactions into statistical mechanical theories or simulations of the OCM.

4. Linearized Poisson-Boltzmann Theory

4.1. Perturbation Expansion and Truncation

Practical applications of PB theory often invoke a perturbation approximation, whereby the microion densities on the right side of the PB equation [Eq. (21)] are expanded in powers of the deviation of the potential from a reference potential. Although not unique, the reference potential is commonly chosen as the reservoir potential ($\psi = 0$) for a suspension in Donnan equilibrium. A more appropriate choice, however, is the mean potential in the suspension $\overline{\psi}$, this being also the only consistent choice for a closed suspension [24, 25, 26, 27, 79]. The distinction between these two choices is especially relevant for deionized suspensions of highly charged colloids.

A linear-screening approximation truncates the expansions of the microion densities at first (linear) order in the potential. Correspondingly, the microion grand potential functional is expanded to quadratic order in the deviations of the microion densities

from their means [26, 27]:

$$\beta\Omega_{\mu}^{\rm lin}[n_{\pm}(\mathbf{r})] = \sum_{i=\pm}\left\{N_i\left[\ln\left(\frac{\bar{n}_i}{n_0}\right)-1\right]+\frac{1}{2\bar{n}_i}\int d\mathbf{r}\,[n_i(\mathbf{r})-\bar{n}_i]^2\right\} + \frac{1}{2}\int d\mathbf{r}\,[n_+(\mathbf{r})-n_-(\mathbf{r})-n_f(\mathbf{r})]\psi(\mathbf{r})\;, \tag{27}$$

where $\bar{n}_{\pm}=N_{\pm}/V'$ here represent the average microion densities in the free volume V' (unoccupied by the macroion hard cores). Minimizing the approximate functional with respect to $n_{\pm}(\mathbf{r})$ now yields the linearized microion density profiles [*cf.* Eq. (20)]:

$$\ln\left(\frac{\bar{n}_{\pm}}{n_0}\right)+\frac{n_{\pm}(\mathbf{r})-\bar{n}_{\pm}}{\bar{n}_{\pm}}\pm\psi(\mathbf{r})=0 \tag{28}$$

and thus

$$n_{\pm}(\mathbf{r})=\bar{n}_{\pm}[1\mp\psi(\mathbf{r})\pm\overline{\psi}]\;, \tag{29}$$

where $\bar{n}_{\pm}=n_0\exp(\mp\overline{\psi})$ for consistency. Substituting Eq. (29) back into Eq. (27) yields the linearized microion grand potential per macroion:

$$\beta\omega_{\mu}^{\rm lin}=\sum_{i=\pm}x_i\left[\ln\left(\frac{\bar{n}_i}{n_0}\right)-1\right]-\frac{Z}{2}\psi(a)+\frac{Z}{2}\overline{\psi}\;, \tag{30}$$

where $x_{\pm}\equiv N_{\pm}/N_m$. The first term on the right side originates from the microion entropy; the second term combines the macroion self energy, $Z^2\lambda_B/(2a)$, and the macroion-counterion interaction energy; and the final term accounts for the average potential energy of the microions relative to the reservoir. Practical implementations aim to calculate the potential.

4.2. Cell-Model Implementation of Linearized Theory

Substituting the linearized microion densities [Eq. (29)] into [Eq. (21)], the linearized PB equation in spherical coordinates takes the form

$$\psi''(r)+\frac{2}{r}\psi'(r)=\kappa^2[\psi(r)-\overline{\psi}]-4\pi\lambda_B(\bar{n}_+-\bar{n}_-)\;,\quad a\le r\le R\;, \tag{31}$$

where $\kappa=\sqrt{4\pi\lambda_B(\bar{n}_++\bar{n}_-)}$ is the screening constant in the suspension. Note that κ depends implicitly on the average macroion density via the global constraint of electroneutrality and that $\kappa^2=\kappa_0^2\cosh\overline{\psi}$ in Donnan equilibrium, but not in closed equilibrium. With cell boundary conditions, $\psi'(a)=Z\lambda_B/a^2$ and $\psi'(R)=0$, the solution of Eq. (31) is

$$\psi(r)=A_1\frac{e^{\kappa r}}{r}+A_2\frac{e^{-\kappa r}}{r}+A_3\;,\quad a\le r\le R\;, \tag{32}$$

where the coefficients are given by

$$A_1=Z\lambda_B\left[(\kappa a-1)e^{\kappa a}-(\kappa a+1)\frac{\kappa R-1}{\kappa R+1}e^{\kappa(2R-a)}\right]^{-1}\;, \tag{33}$$

$$A_2=A_1\frac{\kappa R-1}{\kappa R+1}e^{2\kappa R}\;, \tag{34}$$

$$A_3 = \overline{\psi} + \frac{\bar{n}_+ - \bar{n}_-}{\bar{n}_+ + \bar{n}_-} \ . \tag{35}$$

For a closed suspension, the choice $\psi(R) = 0$ gives a mean potential

$$\overline{\psi} = -A_1 \frac{2\kappa}{\kappa R + 1} \ e^{\kappa R} - \frac{\bar{n}_+ - \bar{n}_-}{\bar{n}_+ + \bar{n}_-} \ . \tag{36}$$

For a Donnan suspension (with zero reservoir potential), averaging Eq. (32) over the free volume of the spherical cell yields rather

$$\overline{\psi} \equiv \frac{3}{R^3 - a^3} \int_a^R \mathrm{d}r \, r^2 \psi(r) = -\sinh^{-1}\left(\frac{3Z}{8\pi n_0 (R^3 - a^3)}\right) \ . \tag{37}$$

The pressure relation [Eq. (22)], although exact in the cell-model implementation of nonlinear PB theory, does not survive linearization. In linearized PB theory, therefore, the pressure must be computed as a thermodynamic derivative of the microion grand potential [Eqs. (27) and (30)]:

$$p = -\left(\frac{\partial \Omega_\mu^{\mathrm{lin}}}{\partial V}\right)_{T, N_m, n_0} = -\frac{1}{4\pi R^2}\left(\frac{\partial \omega_\mu^{\mathrm{lin}}}{\partial R}\right)_{T, n_0} \ . \tag{38}$$

4.3. Effective-Interaction Implementation of Linearized Theory

In contrast to the cell model, effective-interaction implementations of PB theory include microion-induced interactions between macroions in the suspension. Truncating the ideal-gas free energy functional expansion [Eq. (24)] at quadratic order, or the microion density profile expansions [Eq. (25)] at linear order, amounts to neglecting three-body and all higher-order effective interactions. At the mean-field level, such linear-screening approximations predict an effective electrostatic pair potential of Yukawa form,

$$\beta v_{\mathrm{eff}}(r) = Z^2 \lambda_B \left(\frac{e^{\kappa a}}{1 + \kappa a}\right)^2 \frac{e^{-\kappa r}}{r} \ , \quad r \geq 2a \ , \tag{39}$$

and a one-body volume energy [E_v in Eq. (26)] identical in form to the linearized microion grand potential [Eq. (30)]. The electrostatic potential differs, however, from the cell model prediction. In contrast to the solution of the linearized PB equation in the spherical cell model [Eqs. (32)-(35)], linear-response theory [75, 76, 77, 78] and related effective-interaction theories [64, 65, 66] predict

$$\psi(r) = -Z\lambda_B \ \frac{e^{\kappa a}}{1 + \kappa a} \ \frac{e^{-\kappa r}}{r} \ , \quad r \geq a \ , \tag{40}$$

with mean value

$$\overline{\psi} \equiv 4\pi \frac{N_m}{V'} \int_a^\infty \mathrm{d}r \, r^2 \psi(r) = -\frac{\bar{n}_+ - \bar{n}_-}{\bar{n}_+ + \bar{n}_-} = -\frac{3}{(\kappa a)^2} \frac{Z\lambda_B}{a} \frac{\eta}{1 - \eta} \tag{41}$$

for macroion volume fraction $\eta = (4\pi/3)a^3(N_m/V) = 1 - V'/V$. This potential is identical to the solution of the linearized PB equation for a single macroion in a bulk suspension under open boundary conditions: $\psi(r)$ and $\psi'(r) \to 0$ as $r \to \infty$.

Taking care to consistently incorporate density dependence, the effective electrostatic interactions (including the volume energy) may be input into simulations [87] or statistical mechanical theories for the total semigrand potential

$$\Omega = -k_B T \ln \mathcal{Z} = E_v + F_m \ . \tag{42}$$

In linear-response theory, the macroion free energy

$$F_m = -k_B T \ln \left\langle \exp\left(-\beta H_{\rm hs} - \frac{1}{2} \sum_{i \neq j=1}^{N_m} \beta v_{\rm eff}(r_{ij}) \right) \right\rangle_m \ , \tag{43}$$

which includes contributions from the macroion entropy and interactions, can be reasonably approximated by a simple variational approach. First-order thermodynamic perturbation theory with a hard-sphere reference system [88] predicts a macroion free energy per macroion

$$f_m = \min_{(d)} \left\{ f_{\rm hs}(d) + 2\pi n_m \int_d^\infty {\rm d}r \, r^2 g_{\rm hs}(r;d) v_{\rm eff}(r) \right\} \ , \tag{44}$$

where $f_{\rm hs}$ and $g_{\rm hs}$ are the free energy per macroion and radial distribution function, respectively, of the reference system. Minimization with respect to the effective hard-sphere diameter d generates a least upper bound to f_m .

4.4. Charge Renormalization Theory

Linearized PB theory is valid only for bare macroion charges sufficiently low that nonlinear microion screening can be safely neglected. One might conceive of modeling a highly charged suspension simply by combining the cell model solution of the nonlinear PB equation with the linear-screening approximation for the macroion effective pair potential [Eq. (39)]. However, without consistently incorporating nonlinear corrections to the pair and many-body effective interactions [77, 78], such a hybrid approximation would be uncontrolled.

A more consistent and computationally practical synthesis of nonlinear screening and effective interactions invokes the charge renormalization model of Sec. 2.2 to define an effective macroion valence $\tilde{Z}$ within the linear regime. In this scheme, only the $\tilde{N}_\pm$ free microions (with $\tilde{N}_+ - \tilde{N}_- = \tilde{Z} N_m$), are described by a linear-screening approximation, the remaining $Z - \tilde{Z}$ bound counterions (per macroion) renormalizing the bare charge. A theory developed previously for salt-free suspensions [44, 45] is here generalized to salty suspensions.

The electrostatic potential around a dressed macroion of effective valence $\tilde{Z}$ and association shell thickness δ is given from Eq. (40) by

$$\tilde{\psi}(r) = -\tilde{Z} \lambda_B \, \frac{e^{\tilde{\kappa}(a+\delta)}}{1 + \tilde{\kappa}(a+\delta)} \, \frac{e^{-\tilde{\kappa} r}}{r}, \quad r \geq a + \delta \ , \tag{45}$$

with mean value [*cf.* Eq. (41)]

$$\left\langle \tilde{\psi} \right\rangle = -\frac{\tilde{n}_+ - \tilde{n}_-}{\tilde{n}_+ + \tilde{n}_-} \ . \tag{46}$$

Here $\tilde{n}_\pm = \tilde{N}_\pm/[V(1-\tilde{\eta})]$ are mean number densities of free microions, $\tilde{\eta} = \eta(1+\delta/a)^3$ is the effective volume fraction of the dressed macroions, and $\tilde{\kappa} = \sqrt{4\pi\lambda_B(\tilde{n}_+ + \tilde{n}_-)}$ is a renormalized screening constant. From Eqs. (5) and (45), the association shell thickness is now specified by solving

$$\left| \frac{\tilde{Z}\lambda_B}{[1+\tilde{\kappa}(a+\delta)](a+\delta)} + \left\langle \tilde{\psi} \right\rangle \right| = C \tag{47}$$

self-consistently for δ as a function of $\tilde{Z}$, noting that $\tilde{\kappa}$ depends implicitly on $\tilde{Z}$ and δ.

The basic distinction between free and bound counterions implies a corresponding separation of the volume energy per macroion:

$$\varepsilon_v = \omega_{\rm free} + f_{\rm bound} \ . \tag{48}$$

The linear-screening approximation is applied only to the free microions, whose grand potential (per macroion) is approximated by

$$\beta\omega_{\rm free} = \sum_{i=\pm} \tilde{x}_i \left[\ln\left(\frac{\tilde{n}_i}{n_0}\right) - 1 \right] - \frac{\tilde{Z}^2}{2} \ \frac{\tilde{\kappa}\lambda_B}{1+\tilde{\kappa}(a+\delta)} - \frac{\tilde{Z}}{2} \ \frac{\tilde{n}_+ - \tilde{n}_-}{\tilde{n}_+ + \tilde{n}_-} \ , \tag{49}$$

where $\tilde{x}_\pm \equiv \tilde{N}_\pm/N_m$. Note that $\omega_{\rm free}$ has the same form as $\omega_\mu^{\rm lin}$ [Eq. (30)], except that bare parameters are replaced by renormalized parameters and the macroion self energy is omitted, being now associated with the bound counterions.

The bound counterion free energy is approximated by

$$\beta f_{\rm bound} \simeq (Z-\tilde{Z}) \left[\ln\left(\frac{Z-\tilde{Z}}{v_s}\Lambda^3 \right) - 1 \right] + \frac{\tilde{Z}^2\lambda_B}{2a} \ , \tag{50}$$

the first term on the right side being the ideal-gas free energy of the bound counterions in the association shell of volume $v_s = (4\pi/3)[(a+\delta)^3 - a^3]$ and the second term accounting for the self energy of a dressed macroion, assuming the bound counterions to be localized near the macroion surface ($r = a$).

Given a bare valence, the effective valence equalizes the chemical potentials of counterions in the free and bound phases. This condition is equivalent to minimizing the volume energy [Eq. (48)] at fixed temperature and mean microion densities [31, 32, 33]:

$$\left(\frac{\partial \varepsilon_v}{\partial \tilde{Z}} \right)_{T,\bar{n}_\pm} = 0 \tag{51}$$

with $\tilde{Z}$ and δ related by Eq. (47). The resultant effective valence and corresponding shell thickness in turn determine the effective screening constant $\tilde{\kappa}$.

The effective pair potential between dressed macroions is given in terms of the effective valence and screening constant:

$$\beta\tilde{v}_{\rm eff}(r) = \tilde{Z}^2\lambda_B \left(\frac{e^{\tilde{\kappa}a}}{1+\tilde{\kappa}a} \right)^2 \frac{e^{-\tilde{\kappa}r}}{r} \ , \quad r > 2(a+\delta) \ , \tag{52}$$

from which the macroion free energy can be approximated as [cf. (44)]

$$f_m(n_m, \tilde{n}_\pm) = \min_{(d)} \left\{ f_{\rm hs}(n_m, \tilde{n}_\pm; d) + 2\pi n_m \int_d^\infty {\rm d}r \, r^2 g_{\rm hs}(r, n_m; d) \tilde{v}_{\rm eff}(r, n_m, \tilde{n}_\pm) \right\} \ . \tag{53}$$

The hard-sphere fluid functions, $f_{\rm hs}$ and $g_{\rm hs}$, are calculated from the very accurate Carnahan-Starling and Verlet-Weis expressions [88], respectively. In practice, the renormalized system parameters ($\tilde{Z}$, δ, $\tilde{\kappa}$) must be held constant in the variational minimization and in all thermodynamic partial derivatives.

From the total semigrand potential per macroion, $\omega = \varepsilon_v + f_m$, the thermodynamic pressure finally can be calculated via

$$p = n_m^2 \left(\frac{\partial \omega}{\partial n_m} \right)_{T,n_0} = p_{\rm free} + p_m \ , \tag{54}$$

where

$$\beta p_{\rm free} = \tilde{n}_+ + \tilde{n}_- - \frac{\tilde{Z}(\tilde{n}_+ - \tilde{n}_-)\tilde{\kappa}\lambda_B}{4[1+\tilde{\kappa}(a+\delta)]^2} \tag{55}$$

is the (reduced) pressure due to the entropy and energy of the free microions (bound counterions do not contribute directly, since $\tilde{Z}$ and δ are implicitly fixed in the partial derivatives) and

$$\beta p_m = n_m + n_m^2 \beta \left(\frac{\partial f_m}{\partial n_m} \right)_{T,n_0} \tag{56}$$

is the contribution from the entropy and effective macroion interactions. The macroion pressure also can be obtained from computer simulation using the virial theorem, properly generalized to account for the density dependence of the effective pair potential [87].

Application of charge renormalization theory to bulk suspensions requires setting the parameter C in Eqs. (5) and (47) to define the threshold for renormalization at which bare and effective macroion valences begin to differ. Salt-free suspensions afford some freedom to set this threshold. In previous applications [44, 45], the choice $C = 2$ yielded predictions in close agreement with primitive model simulation data for thermodynamic and structural properties of deionized suspensions [89]. For salty suspensions, however, the physical requirement that the coion density be non-negative [$n_-(\mathbf{r}) \geq 0$ in Eq. (29)] constrains $C \leq 1$. Moreover, the presumed exclusion of coions from the association shell (Sec. 2.2) further dictates that $C \geq 1$. Thus, the renormalization threshold is uniquely defined by setting $C = 1$ in the present generalized theory.

5. Results and Discussion

We consider the biologically relevant case of aqueous suspensions at room temperature ($\lambda_B = 0.72$ nm) and restrict attention to monovalent microions, justifying neglect of microion correlations in the mean-field Poisson-Boltzmann theory. Three different implementations of PB theory are here compared: (1) the full nonlinear PB theory in a spherical cell model (PB-cell); (2) linearized PB theory in the cell model with effective (renormalized) valence (LPB-cell); and (3) linearized PB theory in the effective-interaction model (no cell boundaries) with effective valence (LPB-EI). The nonlinear PB equation with spherical cell boundary conditions [Eq. (21)] was solved numerically

by adapting the elegant Mathematica algorithm proposed by Trizac *et al.* [90]. For the linearized PB equation with cell boundary conditions, the electrostatic potential was obtained analytically from Eqs. (32)-(35) and the pressure numerically from Eq. (38). For the effective-interaction model, the macroion free energy was calculated numerically from Eqs. (52) and (53) and the pressure from Eqs. (54)-(56).

Beginning with salt-free suspensions, Figs. 2 and 3 pit PB theory against primitive model simulations [7, 8, 91]. Predictions are compared for the equation of state (pressure or osmotic coefficient) at various electrostatic coupling strengths $\Gamma = \lambda_B/a$. Figure 2 shows results for $Z = 40$ and $0.0222 < \Gamma < 0.7115$, and Fig. 3 for $Z = 60$ and $\Gamma = 0.3245$. All three implementations of PB theory are seen to agree closely with simulation, even well above the renormalization threshold ($Z\Gamma > 5$), the parameter regime of highly charged latex particles and ionic surfactant micelles. The renormalized linearized PB models prove comparable in accuracy to the renormalized jellium model [8, 48]. Previous work [45, 87] confirmed the high accuracy of the variational approximation for the macroion free energy [Eq. (53)] by comparing the LPB-EI model to Monte Carlo simulations of the one-component model with the same effective interactions.

Figure 4 compares theoretical predictions for the equation of state of a highly deionized suspension at low, but non-zero, salt concentration. For this strongly coupled system ($Z\Gamma \simeq 19$), the effective macroion valence is significantly lower than the bare valence (inset). The same three implementations of PB theory give close mutual agreement for the osmotic pressure. In contrast, linearized PB theory with bare macroion valence (no renormalization) yields qualitatively different predictions, including *negative* osmotic pressure at lower volume fractions. This unphysical behaviour confirms previous findings [44, 45] that charge renormalization can profoundly affect thermodynamic properties. When consistently combined with renormalization theory, however, the cell and effective-interaction models are comparably accurate in describing counterion-dominated suspensions.

Turning to suspensions in Donnan equilibrium with an electrolyte reservoir, we explore the influence of reservoir salt concentration n_0 on osmotic pressure. Figure 5 compares predictions for the equation of state of a suspension of highly charged macroions with $a = 50$ nm, $Z = 500$, over a wide range of concentrations. With increasing ionic strength, small relative differences in osmotic pressure for $n_0 < 0.1$ mM grow to significant deviations for $n_0 > 0.4$ mM (Fig. 5a). At concentrations in the range 1 mM $< n_0 <$ 10 mM (Figs. 5b and 5c), a sizeable gap separates the predictions of nonlinear PB theory in the cell model and linearized PB theory in the (charge-renormalized) effective-interaction model. This gap can be traced to the free energy and pressure contributions from microion-induced interactions and correlations between macroions, which are naturally included in the effective-interaction model but omitted from the cell model [92, 93]. Nevertheless, the salt concentrations predicted by the PB-cell and LPB-EI models are in near-exact agreement (inset to Fig. 5c).

At reservoir concentration $n_0 = 1$ mM, the cell-model implementation of linearized PB theory predicts negative osmotic pressure and bulk modulus over a range of volume

fractions. However, since the nonlinear PB-cell model predicts strictly positive pressure and bulk modulus [26, 94], as does the LPB-EI model, this anomalous prediction can only be an artifact of the LPB-cell model at intermediate ionic strengths. At physiological and higher salt concentrations ($n_0 > 100$ mM), microion screening so weakens effective macroion interactions that accuracy of the cell model is restored for the colloidal parameters here studied.

Finally, we revisit the fundamental issue of thermodynamic phase stability. Previous studies based on linearized PB theory [64, 65, 66, 67, 68] and nonlinear response theory [78], without regard for charge renormalization, predicted a spinodal instability in deionized suspensions at low (but nonzero) salt concentrations. Separation into macroion-rich (liquid) and macroion-poor (vapour) phases was predicted in a parameter regime ($Z\lambda_B/a > 7$) that lies slightly beyond the threshold for charge renormalization. Subsequent analysis [24, 25, 26, 27, 94] attributed this unusual instability to an artifact of linearization approximations. The theory of Zoetekouw and van Roij [42, 43], which incorporates an effective macroion valence, yields a revised prediction of instability at much stronger couplings ($Z\lambda_B/a > 24$). This prediction, however, being deduced from a mean-field theory, cannot be directly compared with simulations of salt-free suspensions [5, 7, 9, 12, 14, 15] that exhibit macroion aggregation driven by counterion correlations.

In contrast, the present effective-interaction implementation of linearized PB theory, surveyed over wide ranges of colloidal parameters (a, Z, η) and salt concentrations, predicts no phase instability for any physically rational renormalization threshold ($C \leq 1$). Instability emerges only when the theory is pushed beyond unphysical renormalization thresholds ($C > 1$) that imply negative coion densities. The absence of thermodynamic instability predicted here is consistent with the renormalized jellium model [34, 35], the cell-model implementation of nonlinear PB theory, which admits only a positive bulk modulus [26, 94], and with primitive model simulations for weakly correlated microions [95]. The apparent discrepancy between predictions of the present approach and that of refs. [42, 43] could be related to the different reference potentials chosen for linearization of the PB equation.

6. Conclusions

Summarizing, a theory of charge renormalization that was previously developed for salt-free colloidal suspensions is here generalized to suspensions dialyzed against an electrolyte reservoir. The theory incorporates into the one-component model an effective macroion valence, defined via a simple thermal criterion. Effective electrostatic interactions — one-body volume energy and effective pair potential — are derived from Poisson-Boltzmann theory, via a linear-screening approximation, and depend on the renormalized parameters. In contrast to the salt-free case, the presence of salt ions imposes a unique threshold for charge renormalization.

When applied to salt-free, aqueous suspensions with monovalent counterions,

the renormalized effective-interaction implementation of linearized PB theory predicts osmotic pressures in excellent agreement with the cell-model implementation of nonlinear PB theory and with available data from Monte Carlo simulations of the primitive model. With increasing salt concentration, predictions of the effective-interaction and cell-model implementations increasingly deviate from one another. The deviations are attributed to the relatively large pressure contribution originating from microion-induced effective interactions and correlations between macroions, which are neglected in the cell-model implementation. At physiological and higher salt concentrations, however, the macroions are so strongly screened that the relative deviations are negligible. We conclude that the cell-model implementation of PB theory, although remarkably accurate at relatively low and high salt concentrations, is less reliable at intermediate salt concentrations, roughly in the range 0.5 mM$< c_s <$50 mM. More extensive data from controlled experiments and simulations of the primitive model, especially for bulk suspensions at significant salt concentrations, are required to test the accuracy of competing theories.

The present approach reveals no indication of a liquid-vapour phase instability. Nevertheless, counterion screening in deionized suspensions undoubtedly promotes macroion cohesion, as manifested in the density dependence of the volume energy. Therefore, effective electrostatic interactions, if not driving, may nevertheless assist an instability that is favoured also by other cohesive mechanisms, such as attractive van der Waals or depletion interactions. The complex interplay between such complementary mechanisms for phase separation will be explored in future work.

Acknowledgments

Helpful discussions with Sylvio May and correspondence with Andrey Brukhno, Ramon Castañeda-Priego, Marcus Deserno, and Hans-Hennig von Grünberg are gratefully acknowledged. This work was partially supported by the National Science Foundation (DMR-0204020). Acknowledgment is made to the Donors of the American Chemical Society Petroleum Research Fund (PRF 44365-AC7) for partial support of this research.

[1] D. F. Evans and H. Wennerström, *The Colloidal Domain*, 2nd ed. (Wiley-VCH, New York, 1999).
[2] B. V. Derjaguin and L. Landau, Acta Physicochimica (URSS) **14**, 633 (1941).
[3] E. J. W. Verwey and J. T. G. Overbeek, *Theory of the Stability of Lyophobic Colloids* (Elsevier, Amsterdam, 1948).
[4] P. Linse, *J. Chem. Phys.* **110**, 3493 (1999).
[5] P. Linse and V. Lobaskin, *Phys. Rev. Lett.* **83**, 4208 (1999).
[6] V. Lobaskin and P. Linse, *J. Chem. Phys.* **111**, 4300 (1999).
[7] P. Linse, *J. Chem. Phys.* **113**, 4359 (2000).
[8] R. Castañeda-Priego, L. F. Rojas-Ochoa, V. Lobaskin, and J. C. Mixteco-Sánchez, *Phys. Rev.* E **74**, 051408 (2006).
[9] A. V. Brukhno, T. Åkesson, and B. Jönsson, *J. Phys. Chem.* B, **113**, 6766 (2009).
[10] M. J. Stevens, M. L. Falk, and M. O. Robbins, *J. Chem. Phys.* **104**, 5209 (1996).
[11] E. Allahyarov, I. D'Amico, and H. Löwen, *Phys. Rev. Lett.* **81**, 1334 (1998).
[12] R. Messina, C. Holm, and K. Kremer, *Phys. Rev. Lett.* **85**, 872 (2000).
[13] V. Lobaskin, A. Lyubartsev, and P. Linse, *Phys. Rev.* E **63**, 020401(R) (2001).
[14] V. Lobaskin and K. Qamhieh, *J. Phys. Chem.* B **107**, 8022 (2003).
[15] J. Reščič and P. Linse, *J. Chem. Phys.* **114**, 10131 (2001).
[16] A.-P. Hynninen, M. Dijkstra, and A. Z. Panagiotopoulos, *J. Chem. Phys.* **123**, 84903 (2005).
[17] A.-P. Hynninen and A. Z. Panagiotopoulos, *Phys. Rev. Lett.* **98**, 198301 (2007).
[18] A.-P. Hynninen and M. Dijkstra, *J. Chem. Phys.* **123**, 244902 (2005).
[19] For reviews of colloidal interactions, see C. N. Likos, Phys. Rep. **348**, 267 (2001); L. Belloni, *J. Phys.: Condens. Matter* **12**, R549 (2000); J. P. Hansen and H. Löwen, Annu. Rev. Phys. Chem. **51**, 209 (2000).
[20] J. Israelachvili, *Intermolecular and Surface Forces* (Academic, London, 1992).
[21] M. Deserno and C. Holm, in *Electrostatic Effects in Soft Matter and Biophysics*, vol. 46, NATO Advanced Studies Institute, Series II: Mathematics, Physics and Chemistry, edited by C. Holm *et al.* (Kluwer, Dordrecht, 2001).
[22] R. A. Marcus, *J. Chem. Phys.* **23**, 1057 (1955).
[23] A. R. Denton, in *Nanostructured Soft Matter: Experiment, Theory, Simulation and Perspectives*, ed. A. V. Zvelindovsky (Springer, Dordrecht, 2007).
[24] H. H. von Grünberg, R. van Roij, and G. Klein, Europhys. Lett. **55**, 580 (2001).
[25] R. Klein and H. H. von Grünberg, Pure Appl. Chem. **73**, 1705 (2001).
[26] M. Deserno and H. H. von Grünberg, *Phys. Rev.* E **66**, 011401 (2002).
[27] M. N. Tamashiro and H. Schiessel, *J. Chem. Phys.* **119**, 1855 (2003).
[28] G. S. Manning, *J. Chem. Phys.* **51**, 924 (1969).
[29] F. Oosawa, *Polyelectrolytes* (Dekker, New York, 1971).
[30] S. Alexander, P. M. Chaikin, P. Grant, G. J. Morales, and P. Pincus, *J. Chem. Phys.* **80**, 5776 (1984).
[31] Y. Levin, M. C. Barbosa, and M. N. Tamashiro, Europhys. Lett. **41**, 123 (1998).
[32] M. N. Tamashiro, Y. Levin, and M. C. Barbosa, Eur. Phys. J. B **1**, 337 (1998).
[33] A. Diehl, M. C. Barbosa, and Y. Levin, Europhys. Lett. **53**, 86 (2001).
[34] Y. Levin, E. Trizac, and L. Bocquet, *J. Phys.: Condens. Matter* **15**, S3523 (2003).
[35] E. Trizac and Y. Levin, *Phys. Rev.* E **69**, 031403 (2004).
[36] S. Pianegonda, E. Trizac, and Y. Levin, *J. Chem. Phys.* **126**, 014702 (2007).
[37] T. E. Colla, Y. Levin, and E. Trizac, *J. Chem. Phys.* **131**, 074115 (2009).
[38] K. S. Schmitz, Langmuir **15**, 4093 (1999).
[39] V. Sanghiran and K. S. Schmitz, Langmuir **16**, 7566 (2000).
[40] A. K. Mukherjee, K. S. Schmitz, and L. B. Bhuiyan, Langmuir **18**, 4210 (2002).
[41] D. B. Lukatsky and S. A. Safran, *Phys. Rev.* E **63**, 011405 (2000).
[42] B. Zoetekouw and R. van Roij, *Phys. Rev. Lett.* **97**, 258302 (2006).
[43] B. Zoetekouw and R. van Roij, *Phys. Rev.* E **73**, 21403 (2006).

[44] A. R. Denton, *J. Phys.: Condens. Matter* **20**, 494230 (2008).
[45] B. Lu and A. R. Denton, Commun. Comput. Phys. **7**, 235 (2010).
[46] P. Wette, H. J. Schöpe, and T. Palberg, *J. Chem. Phys.* **116**, 10981 (2002).
[47] T. Gisler, S. F. Schulz, M. Borkovec, H. Sticher, P. Schurtenberger, B. D'Aguanno, and R. Klein, *J. Chem. Phys.* **101**, 9924 (1994).
[48] L. F. Rojas-Ochoa, R. Castañeda-Priego, V. Lobaskin, A. Stradner, F. Scheffold, and P. Schurtenberger, *Phys. Rev. Lett.* **100**, 178304 (2008).
[49] T. Palberg, W. Mönch, F. Bitzer, R. Piazza, and T. Bellini, *Phys. Rev. Lett.* **74**, 4555 (1995).
[50] W. L. Hsin, T.-Y. Wang, Y.-J. Sheng, H.-K. Tsao, *J. Chem. Phys.* **121**, 5494 (2004).
[51] L. Belloni, *Colloids Surf.* A **140**, 227 (1998).
[52] A. Diehl and Y. Levin, *J. Chem. Phys.* **121**, 12100 (2004).
[53] O. Spalla and L. Belloni, *J. Chem. Phys.* **95**, 7689 (1991).
[54] H. H. von Grünberg, J. Coll. Int. Sci. **219**, 339 (1999).
[55] R. Kjellander and D. J. Mitchell, Mol. Phys. **91**, 173 (1997).
[56] H. Löwen, P. A. Madden, and J.-P. Hansen, *Phys. Rev. Lett.* **68** 1081 (1992).
[57] H. Löwen, P. A. Madden, and J.-P. Hansen, *J. Chem. Phys.* **98** 3275 (1993).
[58] H. Löwen and G. Kramposthuber Europhys. Lett. **23** 673 (1993).
[59] R. Tehver, F. Ancilotto, F. Toigo, J. Koplik, and J. R. Banavar *Phys. Rev.* E **59** R1335 (1999).
[60] J. Dobnikar, Y. Chen, R. Rzehak, and H. H. von Grünberg, *J. Chem. Phys.* **119**, 4971 (2003).
[61] J. Dobnikar, D. Haložan, M. Brumen, H. H. von Grünberg, and R. Rzehak, *Comp. Phys. Comm.* **159**, 73 (2004).
[62] For a study of an eccentric PB cell model, see H. H. von Grünberg and L. Belloni, *Phys. Rev.* E **62**, 2493 (2000).
[63] H. Wennerström, B. Jönsson, and P. Linse, *J. Chem. Phys.* **76**, 4665 (1982).
[64] R. van Roij and J.-P. Hansen, *Phys. Rev. Lett.* **79**, 3082 (1997).
[65] H. Graf and H. Löwen, *Phys. Rev.* E **57**, 5744 (1998).
[66] R. van Roij, M. Dijkstra, and J.-P. Hansen, *Phys. Rev.* E **59**, 2010 (1999).
[67] R. van Roij and R. Evans, *J. Phys.: Condens. Matter* **11**, 10047 (1999).
[68] P. B. Warren, *J. Chem. Phys.* **112**, 4683 (2000).
[69] P. B. Warren, *J. Phys.: Condens. Matter* **15**, S3467 (2003).
[70] P. B. Warren, *Phys. Rev.* E **73**, 011411 (2006).
[71] B. Beresford-Smith, D. Y. C. Chan, D. J. Mitchell, J. Coll. Int. Sci. **105**, 216 (1985).
[72] D. Y. C. Chan, *Phys. Rev.* E **63**, 61806 (2001).
[73] D. Y. C. Chan, P. Linse, and S. N. Petris, Langmuir **17**, 4202 (2001).
[74] M. J. Grimson and M. Silbert, Mol. Phys. **74**, 397 (1991).
[75] A. R. Denton, *J. Phys.: Condens. Matter* **11**, 10061 (1999).
[76] A. R. Denton, *Phys. Rev.* E **62**, 3855 (2000).
[77] A. R. Denton, *Phys. Rev.* E **70**, 31404 (2004).
[78] A. R. Denton, *Phys. Rev.* E **73**, 41407 (2006).
[79] A. R. Denton, *Phys. Rev.* E **76**, 051401 (2007).
[80] G. N. Patey, *J. Chem. Phys.* **72**, 5763 (1980).
[81] L. Belloni, *Phys. Rev. Lett.* **57**, 2026 (1986).
[82] S. Khan and D. Ronis, Mol. Phys. **60**, 637 (1987); S. Khan, T. L. Morton, and D. Ronis, *Phys. Rev.* A **35**, 4295 (1987).
[83] M. D. Carbajal-Tinoco and P. González-Mozuelos, *J. Chem. Phys.* **117**, 2344 (2002).
[84] S. N. Petris and D. Y. C. Chan, *J. Chem. Phys.* **116**, 8588 (2002).
[85] J. A. Anta and S. Lago, *J. Chem. Phys.* **116**, 10514 (2002); V. Morales, J. A. Anta, and S. Lago, Langmuir **19**, 475 (2003).
[86] L. B. Bhuiyan and C. W. Outhwaite, *J. Chem. Phys.* **116**, 2650 (2002).
[87] B. Lu and A. R. Denton, *Phys. Rev.* E **75**, 061403 (2007).
[88] J.-P. Hansen and I. R. McDonald, *Theory of Simple Liquids*, 2^{nd} edition (Academic, London,

1986).

[89] In salt-free suspensions, the mean reduced potential [Eq. (46)] is $\langle\tilde{\psi}\rangle = -1$. The choice $C = 2$ in Eqs. (5) and (47), as assumed in refs. [44, 45], then implies a renormalization threshold potential $\tilde{\psi}(a+\delta) = -3$ relative to the reservoir, or $|\tilde{\psi}(a+\delta) - \langle\tilde{\psi}\rangle| = 2$ relative to the mean. The present theory dictates $C = 1$, which proves to maintain comparable accuracy in the salt-free case.

[90] E. Trizac, L. Bocquet, M. Aubouy, and H. H. von Grünberg, *Langmuir* **19**, 4027 (2003).

[91] Note that reduced pressures in Table III of ref. [7] should be $\beta p/n_{\rm tot} = 0.361$ for $Z = 10$, $\Gamma = 1.423$, $\eta = 0.01$; 0.970 for $Z = 40$, $\Gamma = 0.0222$, $\eta = 0.005$; and 0.971 for $Z = 40$, $\Gamma = 0.0222$, $\eta = 0.02$. P. Linse, private communication (2005).

[92] J. Dobnikar, R. Castañeda-Priego, H. H. von Grünberg, and E. Trizac, *New J. Phys.* **8**, 277 (2006).

[93] E. Trizac, L. Belloni, J. Dobnikar, H. H. von Grünberg, and R. Castañeda-Priego, *Phys. Rev.* E **75**, 011401 (2007).

[94] G. Téllez and E. Trizac, *J. Chem. Phys.* **118**, 3362 (2003).

[95] Andrey Brukhno, private communication (2009).

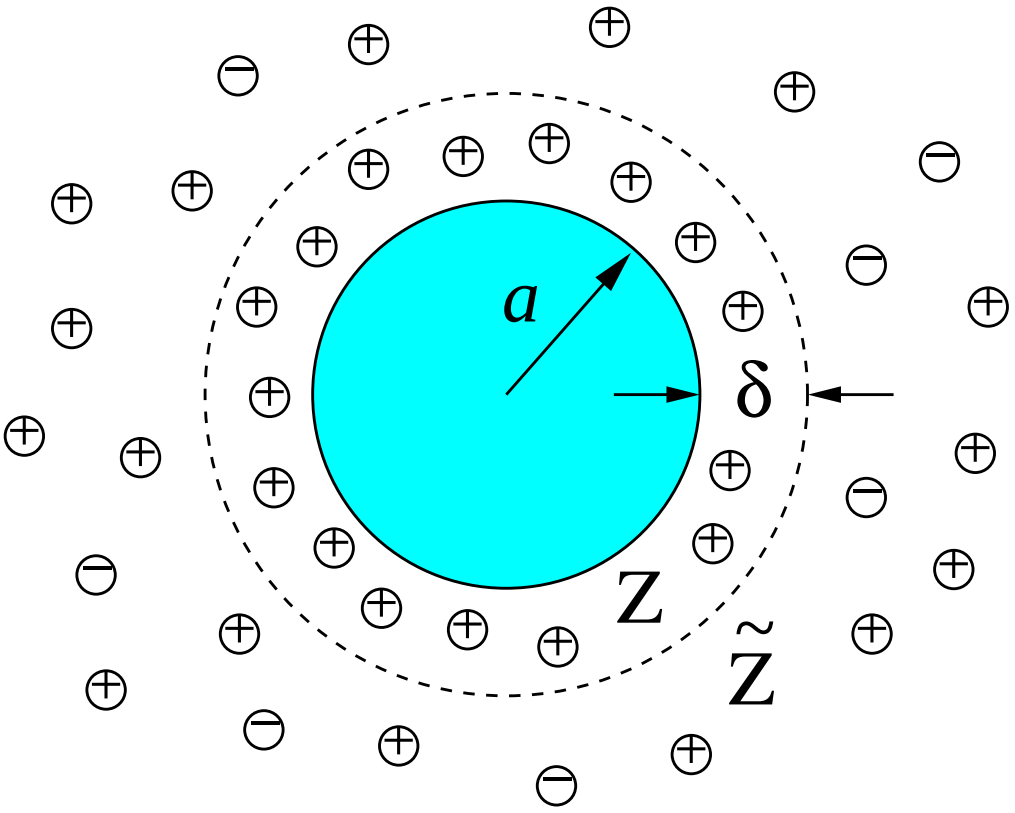

Figure 1. Model of charged colloidal suspension: spherical macroions of radius a and point microions dispersed in a dielectric continuum. Strongly associated counterions in a spherical shell of thickness δ renormalize the bare macroion valence Z to an effective (reduced) valence $\tilde{Z}$.

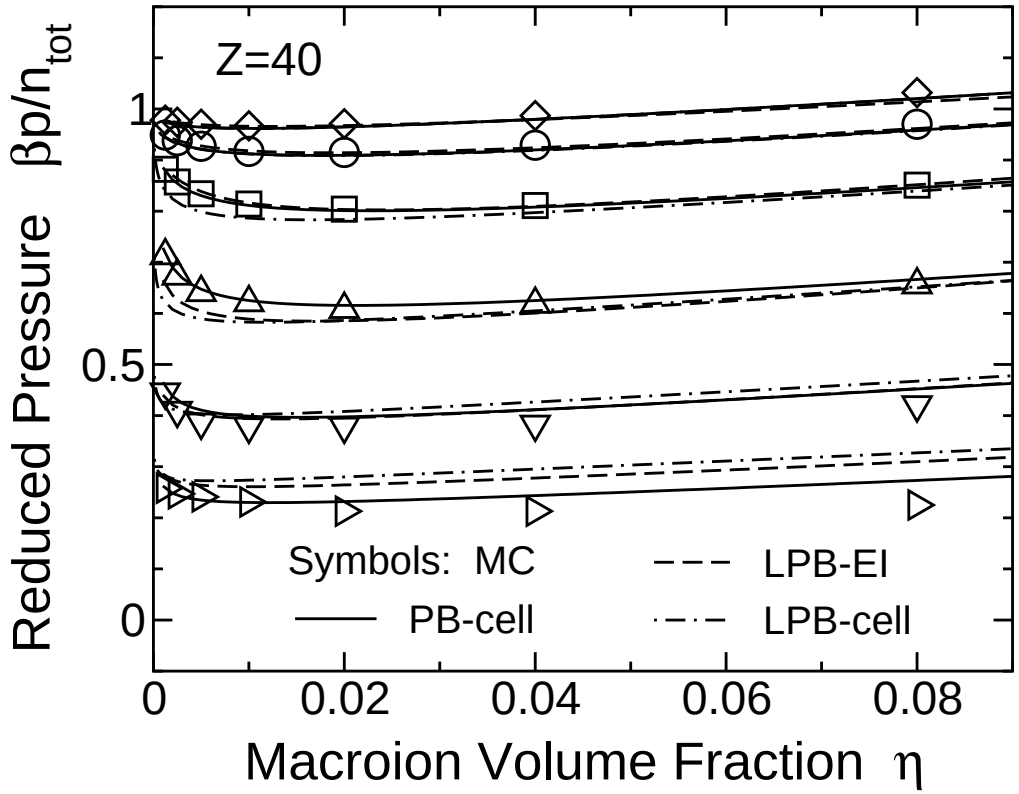

Figure 2. Reduced pressure $\beta p/n_{\rm tot}$ vs. macroion volume fraction η, where $n_{\rm tot} = (Z+1)n_m$ (total ion density), of salt-free suspensions with bare macroion valence $Z = 40$ and electrostatic coupling strengths (top to bottom) $\Gamma = \lambda_B/a = 0.0222$, 0.0445, 0.0889, 0.1779, 0.3558, 0.7115. Symbols: Monte Carlo simulations of the primitive model [7] (symbol sizes exceed error bars). Curves: Poisson-Boltzmann cell model (PB-cell, solid), linearized Poisson-Boltzmann cell model (LPB-cell, dot-dashed), and linearized effective-interaction theory (LPB-EI, dashed). For $\Gamma > 0.1$, the effective macroion charge is renormalized ($\tilde{Z} < Z$).

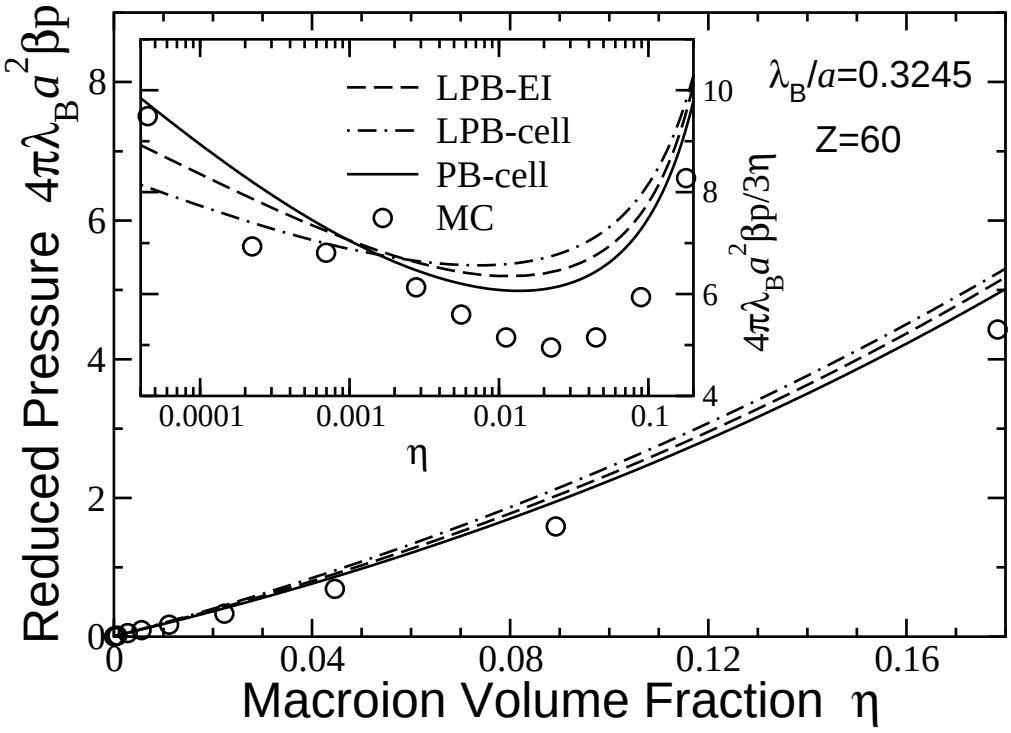

Figure 3. Reduced pressure vs. volume fraction η of a salt-free suspension with bare macroion valence $Z = 60$ and electrostatic coupling strength $\Gamma = \lambda_B/a = 0.3245$. Symbols: Monte Carlo simulations of the primitive model [8]. Curves: Poisson-Boltzmann cell model (PB-cell, solid), linearized Poisson-Boltzmann cell model (LPB-cell, dot-dashed), and linearized effective-interaction theory (LPB-EI, dashed). Inset: osmotic coefficients over several decades of volume fraction.

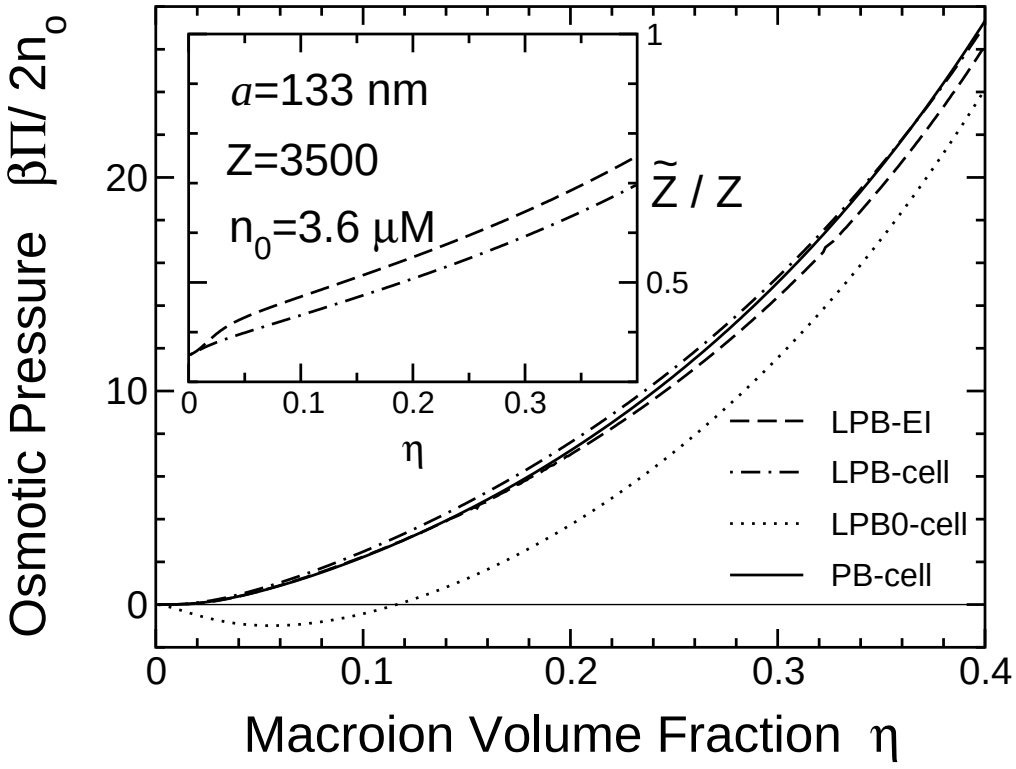

Figure 4. Reduced osmotic pressure vs. volume fraction of a suspension with macroion radius $a = 133$ nm and bare valence $Z = 3500$ in Donnan equilibrium with a salt reservoir of concentration $n_0 = 3.6$ μM. Predictions of alternative theoretical implementations of Poisson-Boltzmann theory are compared: linearized PB theory in the effective-interaction (LPB-EI, dashed) and cell-model (LPB-cell, dot-dashed) implementations, both incorporating charge renormalization; linearized cell model without charge renormalization (LPB0-cell, dotted); nonlinear PB theory in the cell model (PB-cell, solid).

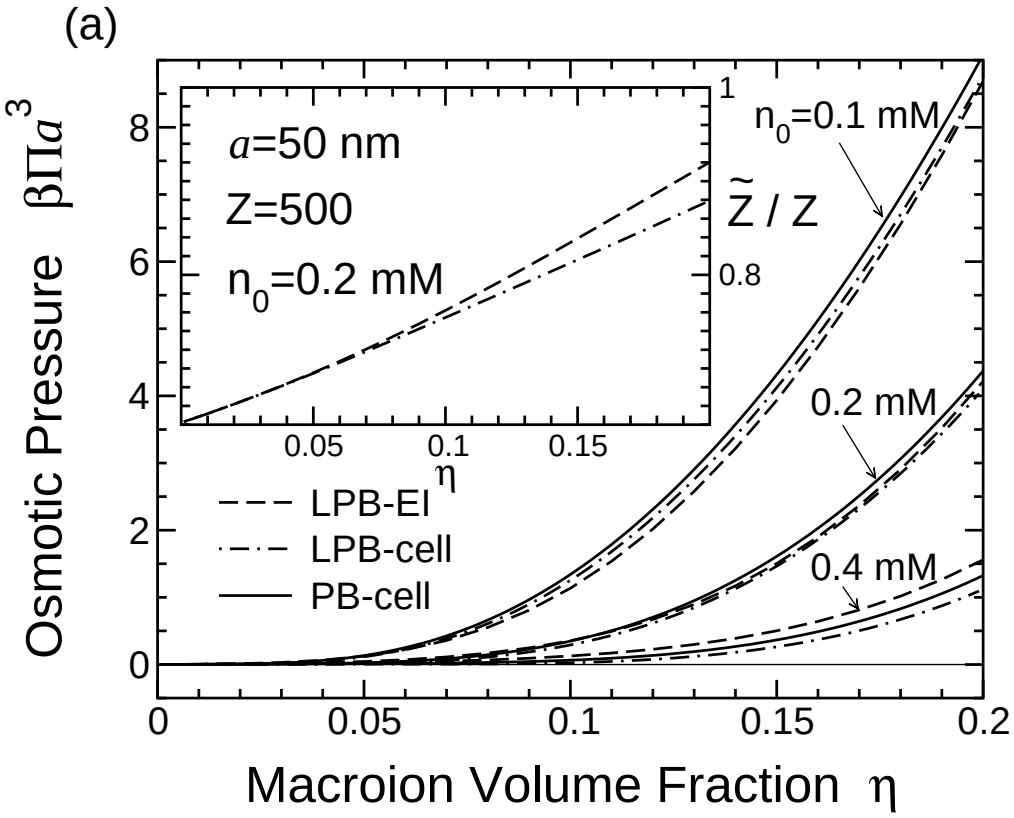
(a)
Osmotic Pressure βΠa^3
Macroion Volume Fraction η
a=50 nm
Z=500
n0=0.2 mM
Z̃ / Z
η
n0=0.1 mM
0.2 mM
0.4 mM
LPB-EI
LPB-cell
PB-cell

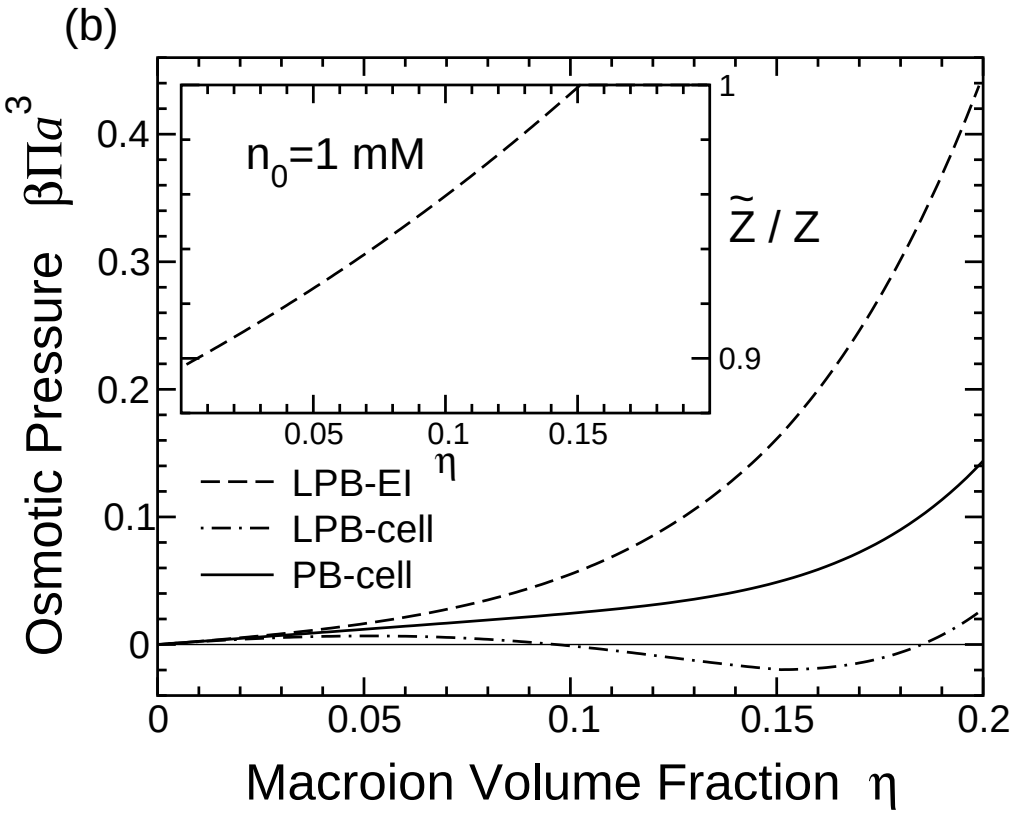
(b)
Osmotic Pressure βΠa^3
Macroion Volume Fraction η
n0=1 mM
Z̃ / Z
η
LPB-EI
LPB-cell
PB-cell

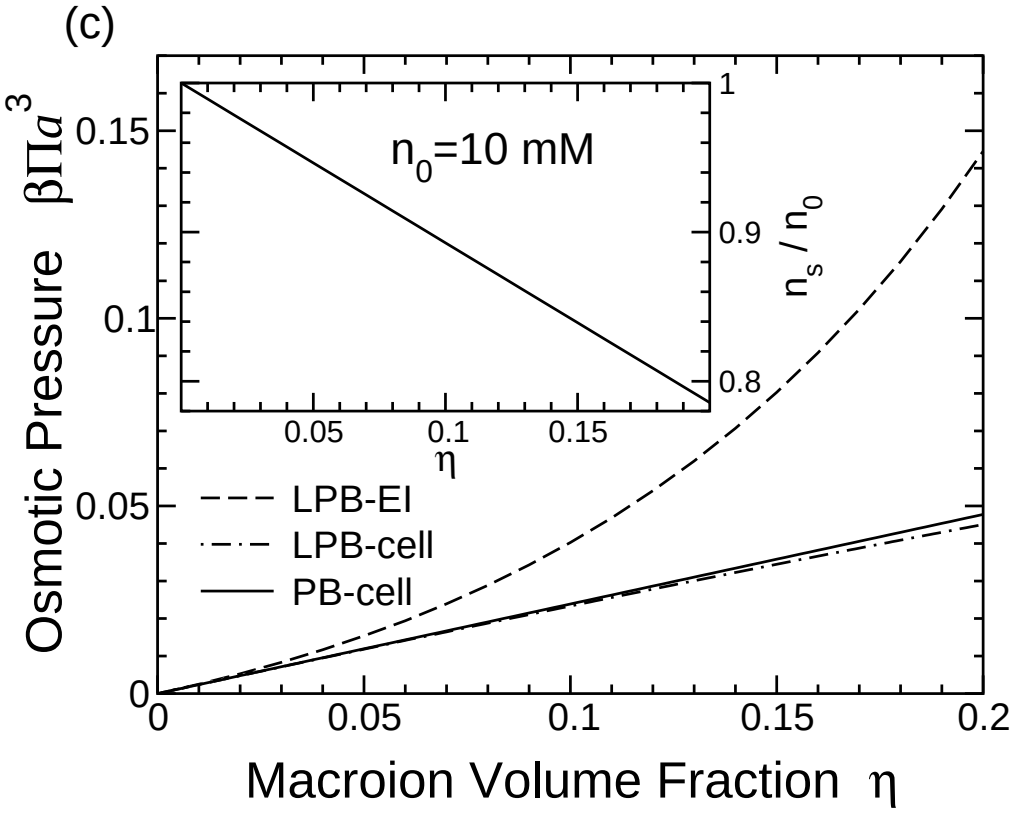

Figure 5. Reduced osmotic pressure vs. volume fraction of a suspension with macroion radius $a = 50$ nm and bare valence $Z = 500$ in Donnan equilibrium with a salt reservoir of various concentrations: $n_0 = 0.1, 0.2, 0.4$ mM (a), 1 mM (b), and 10 mM (c). Predictions of alternative implementations of Poisson-Boltzmann theory are compared: linearized PB theory in the effective-interaction (LPB-EI, dashed) and cell-model (LPB-cell, dot-dashed) implementations; nonlinear PB theory in the cell model (PB-cell, solid). Inset to panels (a) and (b): ratio of effective to bare valence [predictions of the two LPB models are indistinguishable in panel (b)]. Inset to panel (c): ratio of salt concentrations in suspension and reservoir (predictions of the three models are indistinguishable on this scale).